Energy Geoscience 2 (2021) 201–210

Contents lists available at ScienceDirect

Energy Geoscience

journal homepage: www.keaipublishing.com/en/journals/energy-geoscience

Petrography and geochemistry of exported Colombian coals: Implications from correlation and regression analyses

Segun A. Akinyemi [a], Ferney Bohórquez [b], Nazrul Islam [c], Binoy K. Saikia [c], Carlos H. Sampaio [d], Tito J. Crissien [b], Luis F.O. Silva [b, *]

[a] Environmental Remediation & Geopollution Group, Department of Geology, Faculty of Science, Ekiti State University Ado Ekiti, P. M. B. 5363, Ado Ekiti, Nigeria
[b] Department of Civil and Environmental Engineering, Universidad de La Costa, Calle 58 #55-66. 080002, Barranquilla, Atlántico, Colombia
[c] Coal and Energy Group, Materials Science & Technology Division, CSIR-North East Institute of Science & Technology, Jorhat, 785006, India
[d] Departament D'EnginyeriaMinera, Industrial I TIC, Serra Húnter Prof, UniversitatPolitècnica de Catalunya Barcelona Tech, Av. Bases de Manresa 61–63, Manresa, 08242, Barcelona, Spain

ARTICLE INFO

Article history:
Received 14 May 2020
Received in revised form
26 November 2020
Accepted 25 December 2020

Keywords:
Coal characterisation
Geochemistry
Mineralogy
Coal petrology
Colombia

ABSTRACT

The petrology of coal, as determined by the microscopic analysis of organic and inorganic elemental constituents of coal, provides information on its nature and characteristics. Coal is used worldwide in the production of thermal energy and coke. In the case of high-quality Colombian coals, only limited studies have been carried out. The present study presents the geochemical, mineralogical, and petrological characteristics of coal samples collected from Puerto Drummond in Cienaga, Colombia, to predict their potential uses. Therefore, the ultimate, proximate, petrographic, gross calorific value (GCV), ash fusion temperature, Fourier transform infrared spectroscopy (FTIR), X-ray diffraction (XRD), X-ray fluorescence (XRF), and Thermogravimetric (TG) analyses were employed in this study. The petrological analysis reveals that Colombian coals are naturally more abundant in vitrinite (72%) than inertinite (14–23%) macerals. Silicates and aluminosilicate are the main minerals present as fine particles mixed with macerals. The XRD and FTIR analyses show that the most common and dominant minerals are quartz, while gypsum, hematite, calcite and mica occur in lesser amounts. The oxide composition of the coal ashes consists of 51–58% SiO_2 and 18–25% Al_2O_3 as determined by XRF analysis. In correlation and regression analysis, the moisture content shows a reverse correlation with GCV (Regression value of $R^2 = 0.68$). This study helps researchers to comprehend the importance of Colombian coals and presents various techniques for characterisation of coals.

© 2020 Sinopec Petroleum Exploration and Production Research Institute. Publishing services by Elsevier B.V. on behalf of KeAi Communications Co. Ltd. This is an open access article under the CC BY-NC-ND license (http://creativecommons.org/licenses/by-nc-nd/4.0/).

1. Introduction

Colombia has coal reserves of varying quality distributed across the country. The discovered samples reportedly have a high potential to fulfil the public demand for many hundred years (López &Ward, 2008). Coal is considered as a significant source of energy, and it is one of the most essential resources in South and Central America, which ranks the second with its proved reserve of 4.881 Gt (in anthracite and bituminous coal) in the world. The most significant annual coal production in the region is approximately 62.5 Mt, approximately 1.7% of the world's total. The growth of coal production is close to 5% (British Petroleum Company (BP), 2017). The International Energy Agency (IEA) reported that Colombia is the fourth largest coal exporter in the world (IEA, 2017), with most of the coal sourced from the Caribbean Region. The Cesar Department, with a population of 1 million and an area of 22.9 km^2 in the Caribbean Region, is one of the most critical departments in terms of coal production, taking up to 43% of the country's total (Velásquez and Mercedes, 2016). There are two large Carboniferous areas in the Cesar Department, namely, La Jagua de Ibirico and La

* Corresponding author.
E-mail address: felipeqma@hotmail.com (L.F.O. Silva).

Production and Hosting by Elsevier on behalf of KeAi

https://doi.org/10.1016/j.engeos.2020.12.003
2666-7592/© 2020 Sinopec Petroleum Exploration and Production Research Institute. Publishing services by Elsevier B.V. on behalf of KeAi Communications Co. Ltd. This is an open access article under the CC BY-NC-ND license (http://creativecommons.org/licenses/by-nc-nd/4.0/).

Loma. The first is located in the municipality of the same name and is subdivided into two zones: La Jagua and Cerro Largo. The two largest companies that mine these areas are Drummond and Glencore-Prodeco. Their production accounts for nearly 95% of the total production in the department. These companies manage mining and transportation of coal directly from mines to ports located in Cienaga (Magdalena Department) and load vessels for export to Europe, Asia, North, Central and South America (Silva et al., 2012; Drummond, 2017). The lacking of fundamental data for these exported coal deposits has influenced many aspects of utilization and safety related to coal in the country.

Coal petrography is the microscopic and macroscopic representation of coal materials, i.e., the elemental composition, mineral matter; maceral groups, and vitrinite reflectance, which is considered as a rank indicator. There are three macerals: vitrinite, liptinite, and inertinite (Hower et al., 1998; Ao et al., 2012). The petrology of organic and inorganic coals along with coal rank determines coal quality (Hower et al., 1998; Ao et al., 2012). So far, there have been only limited studies on the petrology and geochemistry of coal samples from Puerto Drummond in Cienaga, Colombia.

Therefore, the main objective of the present study is to characterize and evaluate the physico-chemical, petrographic and calorific characteristics of exported Colombian coal through various techniques including proximate, ultimate, ash fusibility temperature, Fourier transform infrared (FTIR) spectroscopy, X-ray diffraction (XRD) spectroscopy, X-ray Fluorescence (XRF) spectroscopy and Thermogravimetric analyses (TGA). The intercorrelation between the physic-chemical characteristics and macerals with the gross calorific value (GCV) of the coals is graphically examined through regression analysis to establish the relationships between these variables and potential applications.

2. Materials and methods

2.1. Sampling

Standard (0 × 50 mm) thermal coal samples (19 samples) were collected at Puerto Drummond in Cienaga, Colombia (Fig. 1A &B). Samples were prepared by using a 5-kg representative split screened through a No. 4-mesh sieve and then divided for each analysis (International Organization for Standardization, 2006).

2.2. Analytical procedures

2.2.1. Chemical analysis

The determination of total moisture of coal samples was carried out in two stages. In the first stage, each sample was crushed to a top size of No. 8 mesh, 2.36 mm, and dried in a drying cabinet (Preiser Scientific Stainless Steel Desiccating Cabinet) at 40 °C. In the second stage, the sample was dried in a drying furnace (Thermo Scientific™ Thermolyne™ Industrial Benchtop Muffle Furnace) at 108 °C for 3 h (International Organization for Standardization, 2008b, International Organization for Standardization, 2010c).

For proximate analysis, each sample was pulverised to a top size of No. 4 mesh, 180 μm, to determine analysis moisture, ash and volatile matter of samples following ISO standard methods (ISO1171:2010; ISO17246: 2010c). The moisture content for the calculation to different bases was determined after drying the sample in a nitrogen atmosphere at 105 °C–110 °C in a drying furnace (Carbolite AAF 1100 Furnace, United Kingdom) (ISO 11722: 2013). For ash determination, the samples were combusted in a muffle furnace (Carbolite) under an air atmosphere starting at ambient temperature (27 °C) up to 500 °C with a rate of 9 °C/min for 90 min after which samples were burned for 90 min more up to 815 °C with a rate of 15 °C/min (ISO1171: 2010). For volatile matter (VM) determination, each sample was heated at 900 °C in a muffle furnace (Carbolite AAF 1100, United Kingdom) without contact with air for 7 min and then cooled at ambient temperature for 7 min and in a desiccator (ISO562: 2010) for another 7 min.

The determination of carbon, hydrogen, and sulphur contents was performed using an ELTRA CHS 580 analyzer (ISO29541: 2010; International Organization for Standardization, 2006b). This consisted of combustion of 250 mg of sample at 1350 °C in an oxygen flow. The CHN contents were then determined using IR spectrometry. The products of combustion are mainly carbon dioxide, water vapour, and sulphur oxides (International Organization for Standardization, 2005).

The determination of the GCV was carried out in a PARR 6200 Isoperibol Calorimeter based on the bomb calorimetric method. Hence, the net calorific value was determined using pure oxygen, water, and benzoic acid as standard and calculated from the heat capacity of the system (ISO 1928: 2009).

The ash fusibility temperature was carried out in a muffle furnace (Carbolite) using a test piece made of coal ash sample heated at 1000 °C and a rate of 10 °C/min up to 1500 °C. The temperatures at which characteristic changes of the form occur were recorded (ISO540: 2008). The crucible swelling number determination was carried out in a Carbolite Model SNF furnace. A coal sample was heated at a temperature of 820 °C in a covered crucible under standard conditions. The obtained coke button was classified in comparison with the standard profile schemes (ISO 501: 2012). Hardgrove grindability index was determined using a Hardgrove grinding machine (Preiser Scientific) at 60 revolutions and a Ro-Tap sieve shaker (W.S. Tyler). The milling index was determined from the granulometric analysis of the milled product referenced to standard test materials in the literature (International Organization for Standardization, 1994).

2.2.2. Organic petrographic analysis

For each coal sample, epoxy-bound particulate pellets (finer than 20-mesh) were prepared to final 0.05 μm polish. Microscopic examination was subsequently carried out on a Leitz Orthoplan microscope at the Center for Applied Energy Research, University of Kentucky, using reflected-light optics and a 50× oil-immersion objective. The maceral identifications of the coal samples were based on the nomenclature of ICCP (ICCP, 1998; ICCP, 2001; Choudhury et al., 2017; Pickel et al., 2017). The mean maximum vitrinite reflectance was measured from 50 points per coal, using polarised light and a 546-nm filter.

2.2.3. Thermal analysis

Thermogravimetric analysis (TG-DTG) was carried out under non-isothermal conditions using the Thermal Analyzer (Model: TGA 701, LECO). For each test, about 25 mg of sample was placed in an alumina crucible and heated from room temperature (RT) to 900 °C based on the non-isothermal heating rate of 10 °C/min in an oxygen environment.

2.2.4. Fourier transform infrared spectroscopy

FTIR analysis was carried out in a PerkinElmer System 2000 apparatus in the range of 4000 cm^{-1} to 400 cm^{-1}. Samples were thoroughly mixed with the Potassium Bromide (KBr) powder in an agate mortar. This was followed by pelletization of the mixture. The FTIR spectra of the coals were subsequently analysed using the software spectrum V-3.02 (Version 3.02.01, PerkinElmer) in advance mode (Choudhury et al., 2017).

Fig. 1. A) Carboniferous mines in Cesar Department. B) Puerto Drummond Terminal in Cienaga municipality.

2.2.5. X-ray diffraction analysis

X-Ray diffraction (XRD) was performed using the X-Ray diffractometer (Rigako, Ultima IV). The resulting X-ray diffraction data of the coal samples were analysed with starting angle set at 2.00° and stopping angle set at 90.00° and step angle 0.02° with a scanning rate of 1 °C/min and target Cu–K α ($\lambda = 1.7902$A°). The library database 'Rigaku PDXL 1.2.0.1' programme was used for the identification of peaks (Saikia et al., 2014).

2.2.6. X-ray fluorescence spectroscopic analysis

The determination of minor and major elements in coal samples was carried out by X-ray fluorescence (XRF) test method specifications (Saikia et al., 2015a,b). Ashed samples were mixed with cellulose as a binder in a weight ratio of 3:0.6 g and then pellets were made by using a VANEOX -25 t manual press. The sample pellets were then analysed using an Epsilon 3XL benchtop spectrometer with Ag anode X-ray tube and 50 μm thin beryllium window for high sensitivity for light elements (Na, Mg, Al, and Si).

3. Results and discussion

3.1. Chemical characteristic of coal

The moisture and ash content of each coal sample expressed on dry basis is shown in Table 1. The total moisture ranges from 6.05 to 16.09%, whereas the ash was in the range from 6.26 to 8.44%. However, other studies observed that the total moisture content of the Venezuelan samples ranges from 1 to 6 wt% (Hackleya et al., 2005). In these studies, total sulphur content was low with a range of 0.57–0.90%, which indicates this type of coal is suitable for energy generation with restrict regulation of sulphur emission. Low-sulphur coals are generally formed in a fluvial environment, while coals with high sulphur content are deposited in the fresh water alkaline environment affected by seawater incursion with effects of differing groundwater conditions, post-depositional, and authigenic mineralization (Kostova, and Isaeva, 2016).

There are two coals with higher calorific value, sample 1440 with 31.15 MJ/kg and sample 1448 with 31.42 MJ/kg, which can be related to their higher volatile matter content, 40.73%, and 40.93%, respectively. The latter is corroborated with samples 1471 and 1472 whose calorific value and volatile matter content are directly proportional.

3.2. Petrographic characteristics of coal

The petrographic data for the investigated coal samples are given in Table 2 while the photomicrographs of representative coal specimens that showed some vital mineral components are depicted in Fig. 2. The coals are characteristically richer in vitrinite than in inertinite macerals with over 70% vitrinite mainly occurring in the form of collodetrinite. Furthermore, about 14–23% inertinite is present mainly in the form of fusinite and semifusinite. However, the samples with high inertinite contents exhibit low proportions of vitrinite and vice-versa. In addition to the macerals, the coal samples also contain 0.5–5.1% of total mineral components. These levels are somewhat low considering the export potential of the coal types, which are beneficiated for this purpose (Khare and Baruah, 2010). Silicates are the main minerals found as fine particles mixed with fragmented macerals (Fig. 2-D) and are attributed to detrital origin (Vassilev and Vassileva, 1996). The Hard grove index (HGI) of most of the coal samples characterize the grinding of the coals and indicator of mill performance. The coals are moderately hard and depend on the vitrinite characteristics as observed above.

3.3. Thermogravimetric properties of coals

The TG-DTG data (Fig. 3) of the coal samples mainly indicate three temperature regions. The DTG curve of all coal samples shows the same trend in temperature regions in having three peaks due to

Table 1
Proximate and ultimate analysis and sulphur content (wt.%) in coal samples of Cienaga, Colombia.

Sample ID.	Total moisture	Inherent moisture	Ash	Volatile matter	Fixed carbon	Total sulphur	Carbon	Hydrogen	Gross calorific value	Hardgrove index
1425	14.94	9.31	7.42	40.30	52.28	0.65	72.94	5.08	29.79	45
1440	6.05	3.41	8.40	40.73	50.88	0.60	75.01	5.48	31.15	43
1441	14.88	10.25	7.30	40.27	52.44	0.74	73.63	5.08	29.90	44
1446	13.99	9.45	7.57	40.10	52.33	0.64	73.71	4.99	29.89	44
1448	7.02	3.80	8.08	40.93	50.99	0.75	74.78	5.65	31.42	44
1449	14.21	9.74	6.79	40.67	52.54	0.79	73.91	5.06	30.17	45
1465	14.37	10.07	6.60	40.62	52.87	0.72	73.92	4.88	30.18	45
1466	15.08	9.82	7.41	40.14	52.45	0.71	72.86	5.07	29.82	44
1467	15.11	9.88	7.69	39.81	52.50	0.77	73.14	5.21	29.73	45
1471	14.32	10.43	8.00	39.66	52.34	0.70	73.14	4.78	29.61	44
1472	13.56	8.65	7.90	40.11	52.00	0.90	72.85	5.00	29.74	45
1474	15.29	8.99	7.44	40.53	52.02	0.83	73.67	4.98	29.90	48
1475	13.99	7.71	7.25	40.40	52.36	0.82	73.68	5.02	30.04	46
1478	16.09	9.92	6.94	39.85	53.21	0.67	74.68	5.09	30.05	46
1493	15.22	9.78	6.46	40.67	52.86	0.62	74.76	5.24	30.11	46
1505	15.42	10.55	6.39	40.47	53.13	0.58	74.17	5.01	30.21	46
1506	14.99	10.26	6.26	40.79	52.95	0.57	74.22	5.16	30.21	46
1508	14.28	8.79	8.44	39.80	51.75	0.72	73.59	5.15	29.71	45
1509	14.31	10.08	8.00	39.96	52.03	0.65	74.14	4.87	29.82	46
5329644	15.98	10.58	6.18	40.03	53.79	0.58	75.01	5.18	30.26	44

Table 2
Petrographic composition (vol%) and vitrinite reflectance (Rv_{max}%) of coal samples.

Sample ID	1409	1425	1427	1438	1440	1446	1448	1449	1465	1466	1467	1471	1472	1493	1505	1506	1508	1510	5329644
Telinite	4.6	5.2	6.4	2.7	3.4	3.3	2.2	2.6	4.6	2.5	4.9	3.3	3.7	3.8	3.5	3.8	3.4	3.7	4.2
Collotelinite	27.8	24.9	36.1	31.4	27.4	21.1	18.3	30.1	30.6	28.8	29.3	34.4	42.1	21.9	9.9	15.6	27.7	21.9	20.3
Total telovitrinite	32.4	30.0	42.4	34.2	30.8	24.4	20.5	32.7	35.1	31.3	34.2	37.7	45.7	25.8	13.3	19.5	31.0	25.6	24.5
Vitrodetrinite	1.8	3.5	2.7	8.5	1.3	7.2	4.8	7.3	3.9	3.9	5.5	3.5	4.3	0.6	3.2	4.2	3.1	3.8	6.3
Collodetrinite	33.6	31.4	21.9	32.7	40.9	32.4	39.6	35.4	23.3	37.7	32.0	30.2	24.4	38.6	44.5	45.8	30.0	39.7	37.0
Total detrovitrinite	35.4	34.8	24.6	41.2	42.2	39.7	44.4	42.7	27.1	41.6	37.4	33.6	28.7	39.2	47.7	50.1	33.1	43.5	43.2
Corpogelinite	3.6	5.2	1.8	3.0	4.5	9.0	5.4	3.9	8.0	2.2	3.9	2.9	3.0	6.5	9.2	2.9	3.7	2.5	6.8
Gelinite	0.8	0.2	0.0	0.2	0.0	0.0	0.0	0.0	1.5	0.1	0.0	0.0	0.0	0.2	0.0	0.1	0.0	0.0	0.0
Total gelovitrinite	4.3	5.4	1.8	3.2	4.5	9.0	5.4	3.9	9.5	2.3	3.9	2.9	3.0	6.7	9.2	3.0	3.7	2.5	6.8
Total vitrinite	72.2	70.3	68.9	78.6	77.5	73.1	70.3	79.3	71.8	75.1	75.5	74.2	77.4	71.7	70.2	72.5	67.8	71.6	74.5
Fusinite	10.9	12.3	12.2	7.7	5.0	10.3	3.9	7.0	8.8	8.6	7.5	8.7	7.9	11.0	8.8	10.8	9.4	11.3	7.5
Semifusinite	7.3	5.6	8.1	4.7	4.4	4.1	7.6	5.5	7.0	7.0	5.4	6.1	6.0	5.9	4.6	5.1	6.5	4.9	4.5
Micrinite	1.4	0.4	0.6	0.8	1.8	1.3	2.8	0.5	1.8	1.0	0.9	1.0	1.3	1.4	1.4	0.9	0.9	0.5	1.1
Macrinite	0.6	0.1	0.0	0.5	1.1	0.4	0.8	0.6	0.7	0.3	0.3	0.7	0.2	1.3	0.6	1.1	1.0	1.0	0.7
Secretinite	0.1	0.0	0.0	0.0	0.1	0.0	0.2	0.0	0.1	0.0	0.0	0.0	0.0	0.1	0.0	0.1	0.1	0.1	0.0
Funginite	0.3	0.1	0.4	0.4	0.4	0.4	0.2	0.2	0.7	0.3	0.2	0.3	0.4	1.0	0.3	0.3	0.9	0.5	0.6
Inertodetrinite	0.9	1.4	1.7	2.1	1.6	5.7	4.0	2.1	1.3	2.7	3.9	1.6	1.2	1.3	3.8	3.4	4.5	3.5	3.5
Total inertinite	21.5	20.0	22.9	16.2	14.4	22.1	19.5	15.8	20.4	20.0	18.1	18.3	17.0	22.0	19.5	21.6	23.3	21.8	17.9
Sporinite	2.4	3.5	3.5	1.9	3.8	2.0	4.1	2.2	4.2	2.4	3.3	3.4	2.1	2.5	3.9	2.4	3.0	3.5	3.2
Cutinite	1.9	1.4	1.5	2.1	1.5	1.4	3.1	1.0	1.4	0.9	1.4	2.2	1.2	1.9	4.3	2.0	2.7	1.2	2.3
Resinite	1.4	1.0	1.0	0.4	0.6	0.7	1.6	0.8	1.1	0.8	0.4	1.0	1.2	1.0	1.6	0.5	1.1	0.4	0.7
Alginite	0.0	0.0	0.0	0.0	0.1	0.0	0.0	0.0	0.1	0.0	0.0	0.0	0.0	0.0	0.0	0.0	0.0	0.0	0.0
Liptodetrinite	0.0	0.9	0.9	0.1	1.0	0.2	0.6	0.1	0.5	0.0	0.3	0.3	0.4	0.4	0.4	0.3	1.1	0.5	0.9
Suberinite	0.3	0.4	0.2	0.1	0.0	0.0	0.1	0.1	0.0	0.1	0.1	0.1	0.3	0.0	0.0	0.0	0.1	0.0	0.1
Exsudatinite	0.0	0.0	0.0	0.0	0.0	0.0	0.0	0.0	0.0	0.0	0.0	0.0	0.0	0.0	0.0	0.1	0.0	0.0	0.0
Total liptinite	6.1	7.2	7.1	4.5	7.0	4.2	9.5	4.2	7.2	4.2	5.6	7.0	5.1	5.8	10.1	5.4	8.0	5.6	7.2
Silicate	0.3	4.8	1.5	0.7	1.4	0.7	0.8	1.0	0.6	0.5	0.8	0.8	0.5	0.8	0.3	0.5	1.3	1.2	0.7
Sulfide	0.3	0.3	0.6	0.7	1.0	0.7	0.5	0.3	0.6	0.8	0.6	0.2	0.4	0.3	0.2	0.5	0.5	0.6	0.1
Carbonate	0.0	0.0	0.0	0.0	0.0	0.0	0.1	0.0	0.0	0.1	0.1	0.1	0.0	0.0	0.0	0.0	0.1	0.1	0.0
Total mineral	0.5	5.1	2.1	1.4	2.4	1.4	1.4	1.3	1.2	1.4	1.5	1.0	0.9	1.2	0.5	1.0	1.9	1.9	0.8
Rmax	0.54	0.48	0.58	0.43	0.58	0.50	0.51	0.49	0.49	0.38	0.52	0.51	0.46	0.54	0.54	0.50	0.56	0.57	0.49
St. Dev.	0.04	0.04	0.04	0.05	0.04	0.05	0.05	0.04	0.05	0.06	0.04	0.05	0.05	0.05	0.04	0.05	0.05	0.06	0.05
Rrandom	0.50	0.45	0.54	0.40	0.54	0.46	0.47	0.46	0.46	0.34	0.47	0.47	0.42	0.51	0.50	0.45	0.50	0.45	0.46
St. Dev.	0.03	0.04	0.04	0.05	0.04	0.05	0.05	0.04	0.05	0.05	0.05	0.05	0.04	0.04	0.05	0.04	0.05	0.05	0.04

the presence of similar chemical bonds in their molecular structures. The first region (Fig. 3.1) occurs between 33-195 °C which indicates the release of moisture content from the coal samples (Huang et al., 1996). The maximum loss of water is observed at 89 °C. The second region occurs between 195 °C and 276 °C, where maximum mass loss occurs due to primary devolatilization and char oxidation (Huang et al., 1996). In the second region of the TGA, the graph shows a lower peak temperature due to the reduction of H-bonding occurs (Sharma et al., 2016).

Furthermore, a double peak can be observed in the DTG curves of all coal samples, which could be attributed to the stepwise release of volatile matter. In the third region, observed from 313 °C to 851 °C, the coals begin to oxidise due to the release of CO, CO_2, and CH_4 from volatile matter (Saikia et al., 2014). In this region, the decomposition of mineral matter (quartz, kaolinite etc.) occurs in coal (Sharma et al., 2016) upon combustion, which starts to decompose in the temperature range of 300–350 °C up to the final temperature of 850–900 °C. The thermal decomposition of coals

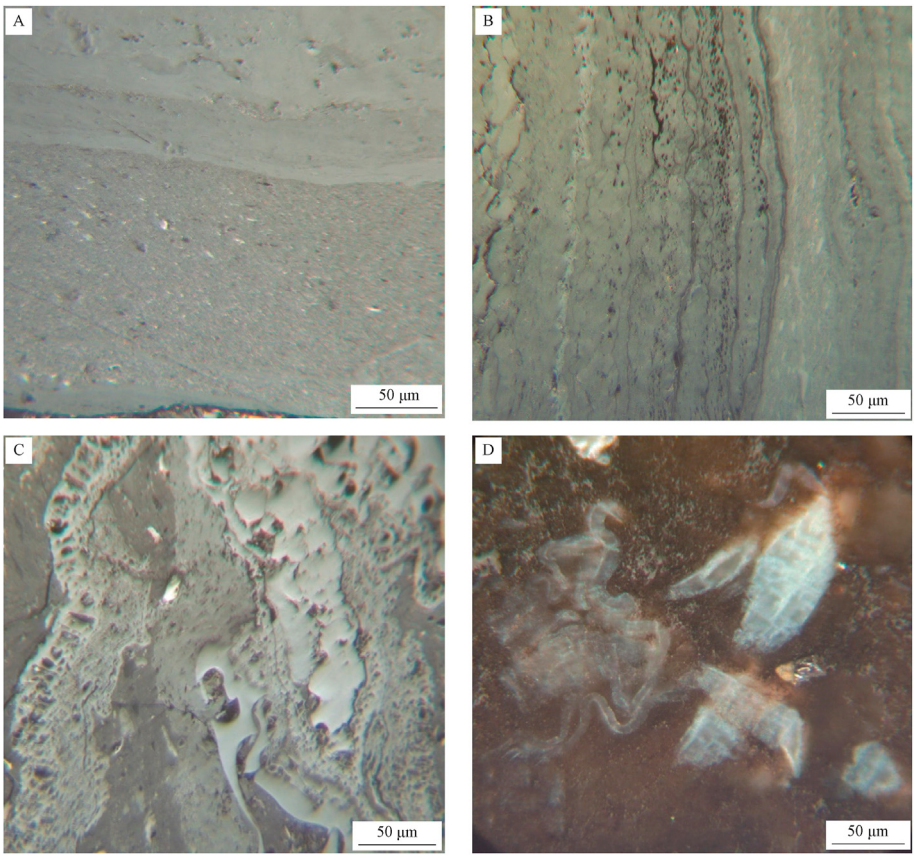

Fig. 2. Polished section photomicrographs of coal components: (A) Vitrinite (1409–17); (B) Liptinite (1409–04); (C) Inertinite (1409–08); (D) Detrital minerals (1409–01).

occurs at a high temperature which leads to the formation of hydrocarbons and tar through the breaking of bonds (Baruah and Khare, 2007; Khare et al., 2011). The maximum loss of volatile matter is observed at 185 °C.These analyses indicate the usefulness of Colombian coals in hard coke making and other industrial purposes (Saikia et al., 2009).

3.4. Functional group analysis

The FTIR spectrum (Fig. 4) of the coal samples reveals sharp peaks in the region of 3000-3600 cm^{-1} due to the stretching vibration of aromatic O–H (phenolic group) and amines (N–H). In this region, the stretching band also indicates the presence of quartz due to the hydroxyl linkage in the clay mineral present in coal (Saikia et al., 2015a,b). The peaks in the 2800-3000 cm^{-1} range indicates the presence of alkane group (C–H). The absorption peak at 2300-2326 cm^{-1} is observed due to the presence of the silane group (S–H) and phosphine (P–H) of the coal samples. The strong absorbance peak occurs at 1506 ± 60 due to stretching of the aromatic C=C ring. Deformation bands (C–H def) occur in the range between 1400-1450 cm^{-1} and the stretching frequency in the range between 1000-1100 cm^{-1} due to the presence of aliphatic ethers and alcohols in various intensity (Khare and Baruah, 2010). This region (1030 ± 30) also indicates the presence of sulfoxide (S=O) and probably some kaolinite minerals in the coal samples (Painter et al., 1981). The absorption peak at 700–900 and 800-1000 cm^{-1} are observed due to the formation of kaolinite, hematite, and illite (Wilson, 1994; Saikia et al., 2015a,b). The stretching bands at 530, 541, and 691 cm^{-1} occur due to S–S bonds of sulfides and the presence of primary and secondary thiols (Khare and Baruah, 2010; Saikia et al., 2015a,b). The peaks at 468 and 472 are assigned to the stretching vibration of sulphonamide (S–N). The absorption peak at 650 ± 10 reveals the presence of chlorite and the peak at 472 indicates the presence of montmorillonite (Speight, 1983). The clay particles act as catalyst during the cracking of volatile matter which cannot be adsorbed on coal on cooling (Saxby et al., 1992).

3.5. XRD-mineralogy

The presence of minerals in the coal samples and their qualitative assessment were carried out by X-ray diffraction. The minerals are identified in the coal samples based on the *d*-spacing values of the XRD peaks (Dutta et al., 2017) (Table 3). The coal samples show the presence of quartz, gypsum, hematite, calcite, and mica, as presented in Fig. 5. Quartz is the standard and dominant mineral present in all the samples except for sample 105 and sample 1446. A prominent peak of quartz is observed in most of the samples due to its high stability (Dutta et al., 2017). Similarly, quartz and hematite were also present in the FTIR analysis of coal samples. The detailed assignments of theta and *d*-values for the detection of minerals are shown in Table 3.

3.6. Coal ash analysis

The chemical composition (%) of the coal ashes were determined by XRF analysis as presented in Table 4. The results indicate that the coal ash is largely composed of 51–58% of SiO_2 and 18–25% of Al_2O_3. Furthermore, the ash also contains low percentages of Mn_3O_4, P_2O_5, SrO, and BaO. The presence of 9–12% of Fe_2O_3 along with pyrite and jarosite occurs in the coals from the northern

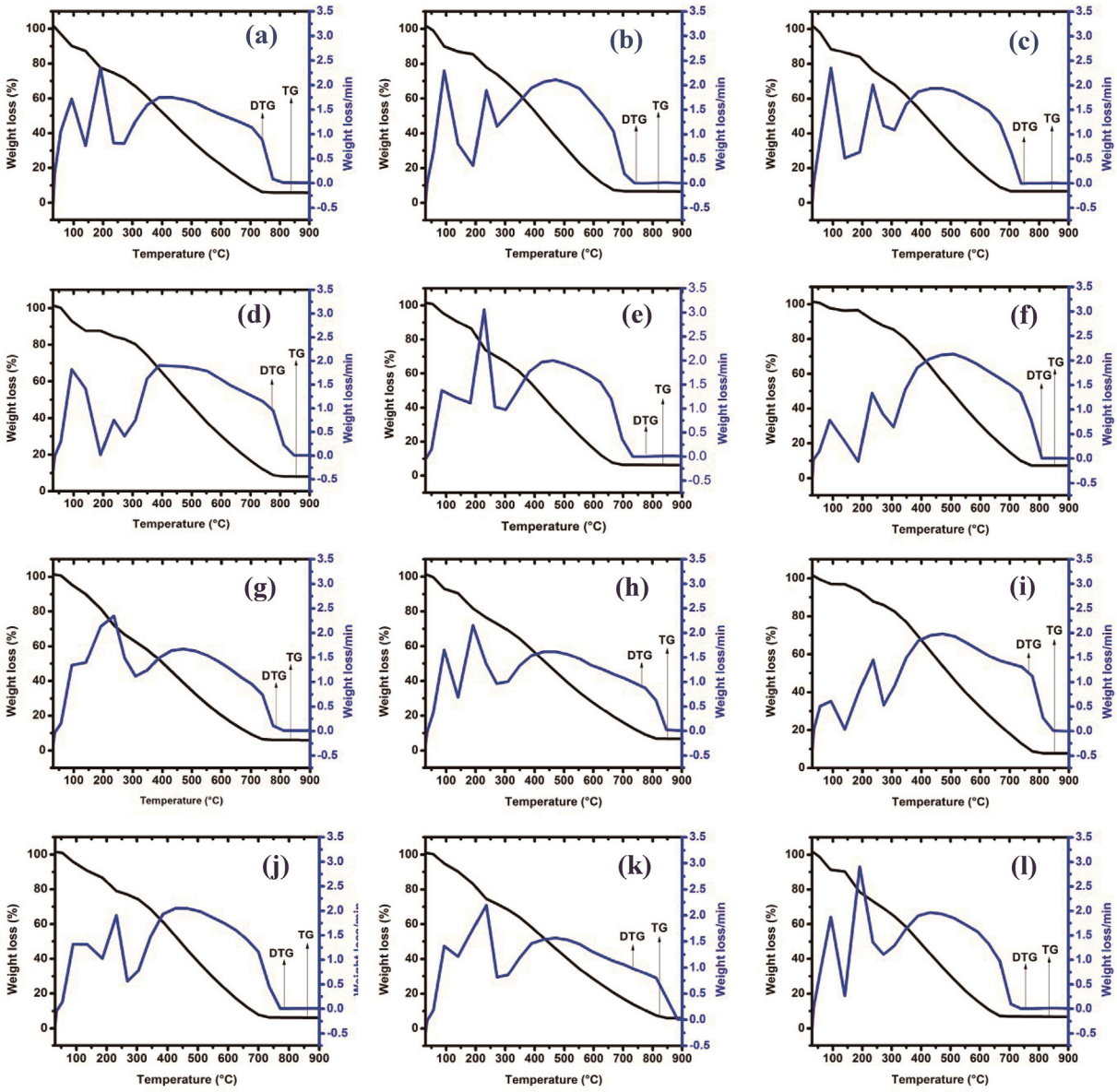

Fig. 3. TG-DTG spectra of coal samples showing the thermal properties of the coals [(a)-105, (b)-1409, (c)- 1425, (d)- 1427, (e)- 1438, (f)-1440, (g)- 1442, (h) – 1446, (i)- 1448, (j) – 1449, (k) – 1465, (l) – 1466].

Colombian mines (López and Ward, 2008). The proportion of CaO in the coal ashes varies from 2 to 4.7% which may be due to the presence of organic matter bound in the clay minerals. The proportion of sulphur as SO_3 retained in the ash varies over 1–5.7%. This is attributed to variation in the proportion of pyrite in the feedstock coals.

3.7. Correlation and regression analysis

The relationship between the macerals (or chemical characteristics) with the gross calorific value (GCV) of the coals was examined by numerical analysis. The statistical variance was computed to establish the numerical relationships between each chemical constituent of the coal samples. Consequently, the interrelationships between the maceral/chemical properties (comprised of the volatile matter, moisture, fixed carbon, ash, vitrinite, inertinite, mineral matter, and ash) and the GCV of coal samples was examined and plotted as presented in Fig. 6.

As observed, the relationship between volatile matter on dry basis and GCV is characterized by an R^2 value of 0.4942, which indicates a good measure of maturity or high coal rank. However, the moisture contents show a reverse correlation with GCV (R^2 = 0.6754). In comparison, the analysis of US coal samples revealed negative effect or weakly correlation between the moisture content and GCV. This parameter evidently indicates slow ranks of the coal due to the diluents related to GCV (Mesroghli et al., 2009). In this study, the bivariate plots show there is no relationship with r squared values all below 0.2.

4. Conclusions

The study presented an overview of the geochemical, mineralogical, and petrographic characteristics of Colombian coals. The chemical and petrographic characteristics of coal can be used as a first-rate indicator of their potential for combustion, liquefaction, and coke production. From these investigations, the Colombian

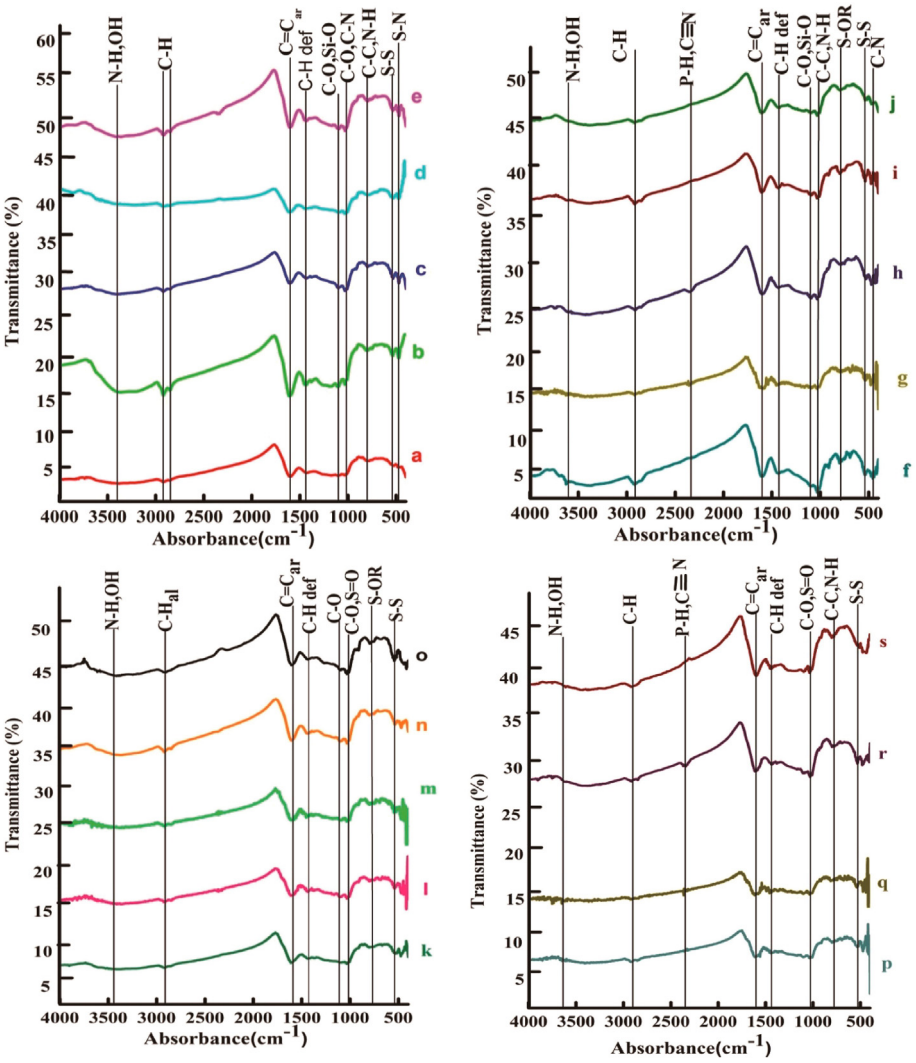

Fig. 4. FTIR spectra of coal samples showing presence of functional groups [(a)-105, (b)-1409, (c)- 1425, (d)- 1427, (e)- 1438, (f)-1440, (g)- 1442, (h) – 1446, (i)- 1448, (j) – 1449, (k) – 1465, (l) – 1466, (m) – 1467, (n) – 1472, (o) – 1493, (p)– 1508, (q) – 1506, (r) – 1510, (s) –5329644].

Table 3
Assignments of XRD d-values for the detection of mineral phases.

Samples	2θ	d-value	Possible minerals	Samples	2θ	d-value	Possible minerals
a	20.8	4.958476835	Quartz	l	12.42	8.274718346	Gypsum
	26.56	3.896651967	Quartz.		26.82	3.85955911	Quartz
c	12.34	8.328153653	Gypsum		50.48	2.099149084	Quartz, hematite
	26.62	3.888027156	Quartz.	m	21.12	4.884181773	Quartz
d	18.46	5.58049251	Quartz		26.88	3.85110209	Quartz
	26.82	3.85955911	Quartz		50.25	2.108128994	Quartz, hematite
e	12.7	8.093006647	Gypsum	n	17.88	5.759971493	Quartz
	21.02	4.907154588	Quartz	o	26.56	3.896651967	Quartz
	26.84	3.856735862	Quartz	p	26.3	3.934485167	Quartz
	50.4	2.102262881	Quartz, hematite	q	12.38	8.301349505	Gypsum
f	21.02	4.907154588	Quartz		20.8	4.958476835	Quartz
	26.84	3.856735862	Quartz		26.56	3.896651967	Quartz
	68.28	1.594926873	Calcite, quartz, hematite	r	12.4	8.288012407	Gypsum
g	26.56	3.896651967	Quartz		20.8	4.958476835	Quartz
l	26.82	3.85955911	Quartz,		26.8	3.862386613	Quartz
j	21.08	4.893344592	Quartz		50.16	2.111666143	Quartz, hematite
	26.82	3.85955911	Quartz		68.52	1.590019174	Calcite, quartz. hematite
	50.4	2.102262881	Quartz, hematite	s	12.34	8.328153653	Gypsum
	68.4	1.592468369	Calcite, quartz. Hematite		20.62	5.001286983	Quartz
k	8.98	11.4338489	Mica		26.56	3.896651967	Quartz,
l	12.42	8.274718346	Gypsum				

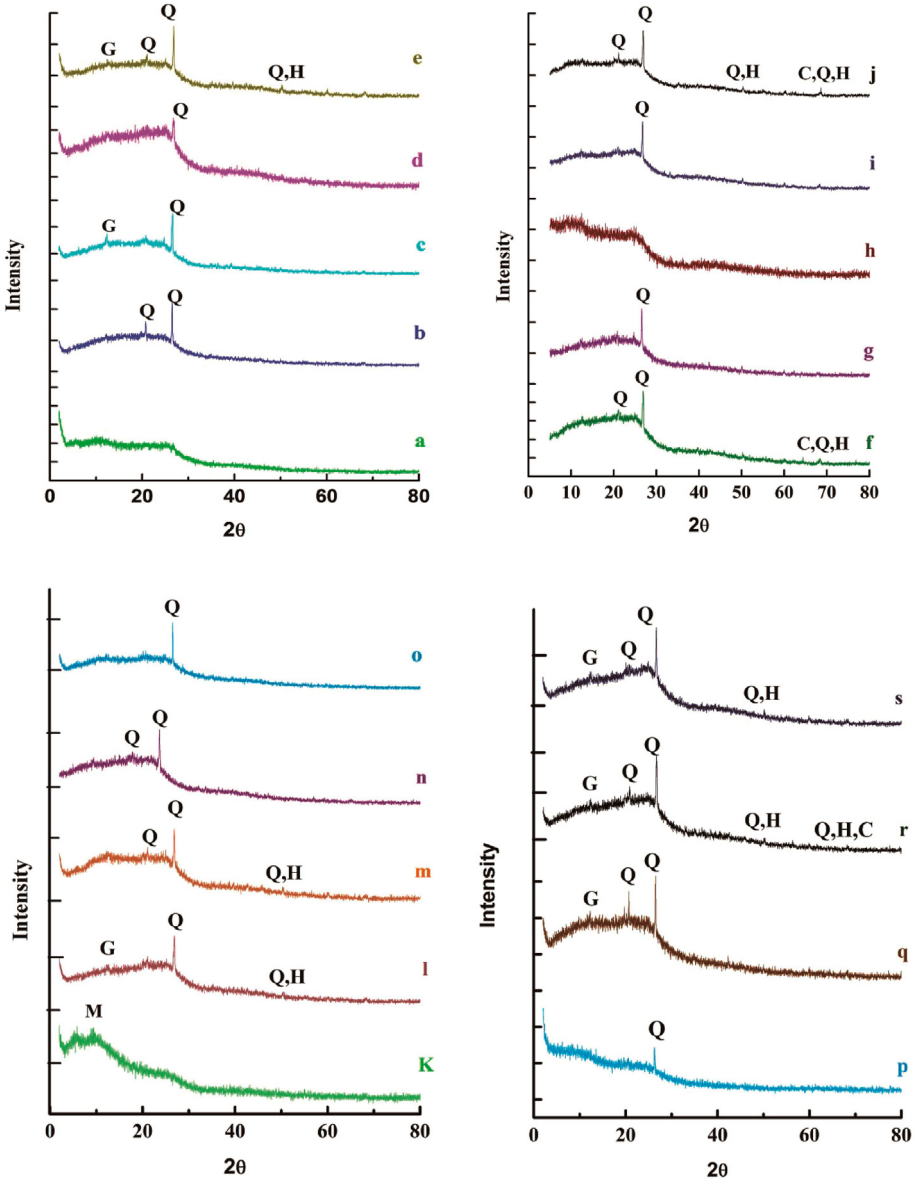

Fig. 5. XRD analysis of coal samples showing the mineral phases in the coals [(a)-1427, (b)-1446, (c)- 1448, (d)- 1493, (e)- 1510, (f)-105, (g)- 1438, (h) – 1440, (i)- 1442, (j) – 1508, (k) – 1409, (l) – 1425, (m) – 1449, (n) – 1465, (o) – 5329644, (p)– 1466, (q) – 1467, (r) – 1472, (s) –1506] [Q-quartz, H- hematite, G-gypsum, C- calcite, M-mica].

Table 4
Major element composition of coal ashes (815 °C) by XRF spectrometry (wt.%).

Sample No.	SiO_2 %	Al_2O_3 %	Fe_2O_3 %	TiO_2 %	Mn_3O_4 %	CaO %	MgO %	Na_2O %	K_2O %	P_2O_5 %	SO_3 %	SrO %	BaO %
1425	52.81	19.56	10.60	0.95	0.07	3.67	1.60	2.63	1.93	0.22	5.51	0.13	0.33
1440	56.64	25.33	9.09	1.57	0.09	2.55	0.70	0.45	1.10	0.14	2.20	0.03	0.14
1441	54.86	19.33	11.62	0.97	0.08	3.95	1.64	2.30	2.00	0.20	2.56	0.15	0.37
1446	54.91	20.31	9.34	1.03	0.06	3.28	1.46	2.64	2.06	0.25	4.21	0.14	0.34
1448	58.00	24.24	9.72	1.44	0.06	2.61	0.80	0.46	1.22	0.14	1.16	0.05	0.13
1449	55.76	19.72	11.74	1.06	0.06	3.26	1.48	2.41	2.29	0.19	1.52	0.16	0.39
1465	54.66	18.70	12.52	1.07	0.09	3.75	1.67	2.43	2.29	0.19	2.11	0.15	0.37
1466	53.70	19.33	10.82	0.98	0.07	3.56	1.67	2.78	2.21	0.23	4.19	0.15	0.36
1467	54.48	20.08	9.97	1.05	0.07	3.60	1.67	2.38	2.15	0.25	3.87	0.14	0.34
1471	55.33	20.61	9.82	1.06	0.06	3.08	1.54	2.46	2.25	0.23	3.12	0.13	0.33
1472	54.14	20.01	12.33	0.99	0.06	2.68	1.48	2.56	2.28	0.20	2.81	0.13	0.35
1474	53.78	20.77	11.42	1.00	0.06	2.99	1.54	2.48	2.24	0.21	3.07	0.14	0.33
1475	54.67	21.02	11.17	1.01	0.05	2.53	1.42	2.47	2.29	0.21	2.73	0.13	0.33
1478	52.41	19.54	10.20	0.98	0.06	3.68	1.66	2.90	2.09	0.26	5.73	0.16	0.37
1493	51.49	19.18	10.83	1.06	0.07	4.68	1.89	2.96	1.97	0.25	5.05	0.18	0.41
1505	52.55	19.21	10.24	0.97	0.07	4.40	1.81	2.71	2.00	0.24	5.27	0.17	0.38
1506	52.43	19.51	10.06	1.02	0.07	4.32	1.81	3.00	1.99	0.25	4.99	0.17	0.38
1508	56.04	20.56	9.81	1.08	0.06	2.74	1.52	2.22	2.32	0.23	2.97	0.13	0.32
1509	55.50	20.14	9.70	1.05	0.06	3.10	1.52	2.50	2.23	0.23	3.48	0.15	0.35
5329644	51.60	18.81	10.47	0.97	0.06	4.63	1.73	3.61	1.99	0.28	5.12	0.24	0.50

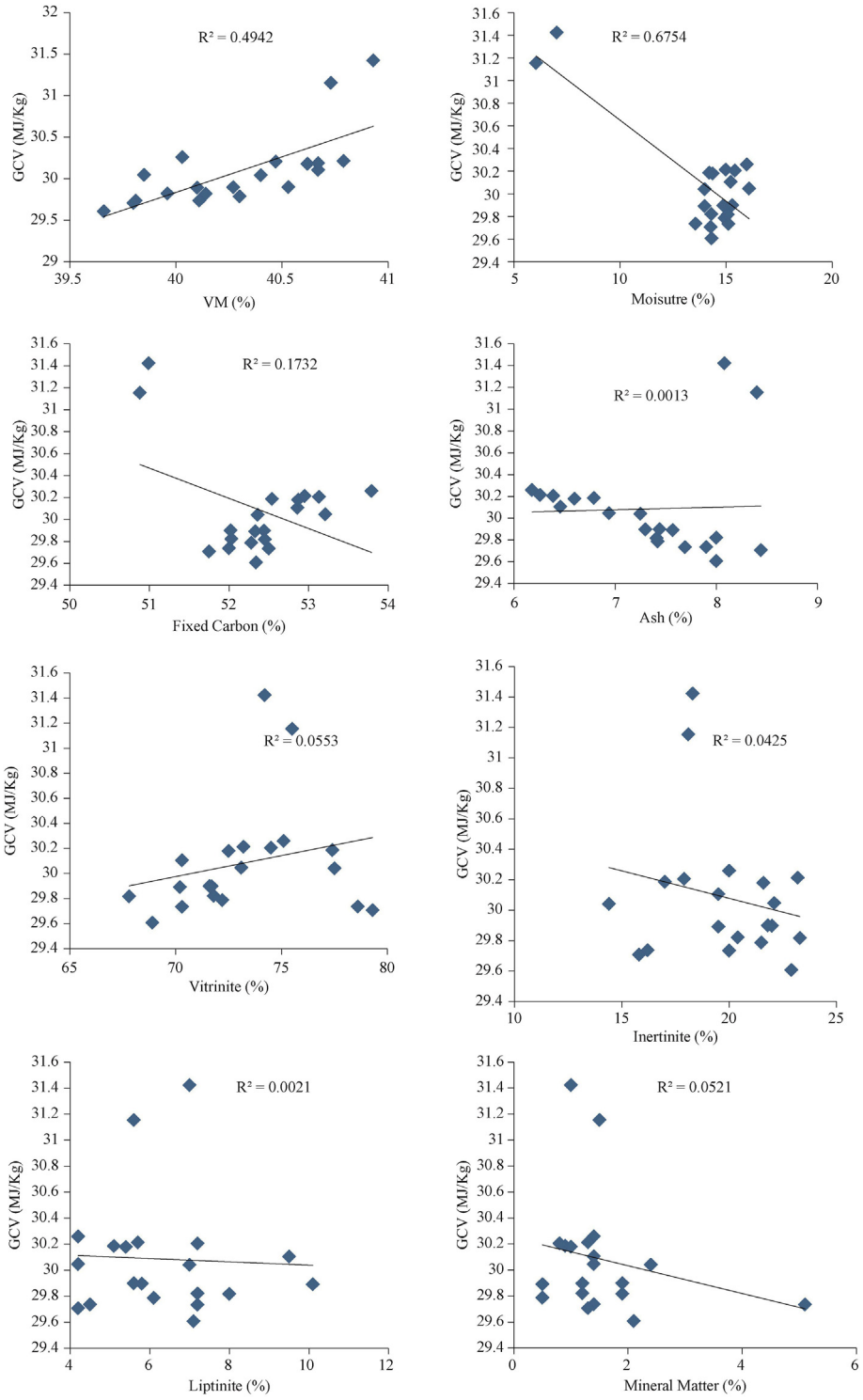

Fig. 6. Relationship of chemical characteristics of coal and macerals with GCV.

coals are vitrinite-rich as the samples contain 0.5–5% of visible mineral components. Silicates were found to be major minerals, and exist as fine particles with partial detrital origin. However, the major minerals identified by XRD and FTIR analyses were quartz, gypsum, hematite, calcite, and mica. Based on the results, the coal samples examined are potentially suitable for energy generation, provided there is strong regulation of sulphur due to the presence of low-sulphur content (0.57–0.90%). The intercorrelation between the chemical characteristics and GCV of the coals reveals that higher moisture content adversely affects the GCV of Colombian coals, based on its reverse correlation with GCV ($R^2 = 0.6754$). Likewise, the macerals (vitrinite, inertinite, liptinite and mineral matter) show poor correlation with GCV ($R^2 = 0.0553$; $R^2 = 0.0425$; $R^2 = 0.0021$; $R^2 = 0.0521$). The results of this petrographic analysis will be helpful in further investigation on the relationship between GCV and coal quality. It is envisaged that the findings of the present

study will motivate further research studies on the characterisation and utilization of Colombian coals in the nation's scientific community.

Declaration of competing interest

The authors declare that they have no conflict of interest.

Acknowledgements

Authors express special thanks to Director (CSIR-NEIST) for this collaboration and Dr Jim C. Hower from the Center for Applied Energy Research (CAER) for the University of Kentucky for technical assistance with the petrology analyses.

References

Ao, W., Huang, W., Weng, C., Xiao, X., Liu, D., Tang, X., Chen, P., Zhao, Z., Wan, H., Finkelman, R.B., 2012. Coal petrology and genesis of jurassic coal in the ordos basin, China. Geosci Front. 3, 85–95.

Baruah, B.P., Khare, P., 2007. Pyrolysis of high sulphur Indian coals. Energy Fuel. 21, 3346–3352.

British Petroleum Company (Bp), 2017. Statistical Review of World Energy. British Petroleum Company, London.

Choudhury, R., Saikia, J., Saikia, B.K., 2017. Mineralogical and ash geochemical studies of coal-mine shale and its hydrocarbon potential: a case studies of shale from makum coalfield. Northeast India. J. Geol. Soc. India 90.

Drummond, Ltd, 2017. Drummond cerróaño record en exportaciones. con más de 32.6 millones de toneladas de carbónenviadas a 24 países. http://www.drummondltd.com. http://www.drummondltd.com/drummond-cerro-ano-record-en-exportaciones-con-mas-de-326-millones-de-toneladas-de-carbon-enviadas-a-24-paises/.

Dutta, M., Saikia, J., Taffarel, S.R., Waanders, F.B., Medeiros, D., Cutruneo, C.M.N.L., Silva, L.F.O., Saikia, B.K., 2017. Environmental assessment and nano-mineralogical characterization of coal overburden and sediment from Indian coal mining acid drainage. Geosci. Front. 1–3.

Hackleya, P.C., Warwicka, P.D., Gonzalez, E., 2005. Petrology, mineralogy and geochemistry of mined coals, western Venezuela. Int. J. Coal Geol. 63, 68–97.

Hower, J.C., Graham, U.M., Wong, A.S., Robertson, J.D., Haeberlin, B.O., Thomas, G.A., Schram, W.H., 1998. Influence of flue-gas desulfurization systems on coal combustion by-product quality at Kentucky power stations burning high-sulfur coal. Waste Manag. 17, 523–533.

Huang, H., Wang, K.Y., Klein, M.T., Calkins, W.H., 1996. Determination of coal rank by thermogravimetric analysis. Fuel Energy Abstr. 37, 170.

IEA, 2017. Coal Information. OECD Publishing, Paris.

International Committee for Coal and Organic Petrology (ICCP), 2001. New inertinite classification (ICCP system 1994). Fuel 80, 459–471.

International Organization for Standardization, 1994. Hard Coal – Determination of Hardgrove Grindability Index (ISO Standard No. 5074).

International Committee for Coal Petrology (ICCP), 1998. The new vitrinite classification (ICCP System 1994). Fuel 77 (5), 349–358.

International Organization for Standardization, 2005. Coal – Ultimate Analysis (ISO Standard No. 17247).

International Organization for Standardization, 2006. Hard Coal and Coke – Manual Sampling (ISO Standard No. 18283).

International Organization for Standardization, 2006b. Solid Mineral Fuels – Determination of Sulfur by IR Spectrometry (ISO Standard No. 19579).

International Organization for Standardization, 2008. Hard Coal and Coke – Determination of Ash Fusibility (ISO Standard No. 540).

International Organization for Standardization, 2008b. Hard Coal – Determination of Total Moisture (ISO Standard No. 589).

International Organization for Standardization, 2009. Solid Mineral Fuels – Determination Gross Calorific Value by the Bomb Calorimetric Method and Calculation of Net Calorific Value (ISO Standard No. 1928).

International Organization for Standardization, 2010. Solid Mineral Fuels – Determination of Ash (ISO Standard No. 1171).

International Organization for Standardization, 2010b. Solid Mineral Fuels – Determination of Total Carbon. Hydrogen and Nitrogen Content – Instrumental Method (ISO Standard No. 29541).

International Organization for Standardization, 2010c. Coal – Proximate Analysis (ISO Standard No. 17246).

International Organization for Standardization, 2010d. Hard Coal and Coke – Determination of Volatile Matter (ISO Standard No. 562).

International Organization for Standardization, 2012. Hard Coal – Determination of Crucible Swelling Number (ISO Standard No. 501).

International Organization for Standardization, 2013. Solid Mineral Fuels – Hard Coal – Determination of Moisture in the General Analysis Test Sample by Drying in Nitrogen (ISO Standard No. 11722).

Khare, P., Baruah, B.P., Rao, P.G., 2011. Application of chemometricsto study the kinetics of coal pyrolysis: a novel approach. Fuel 90, 3299–3305.

Khare, P., Baruah, B.P., 2010. Structural parameters of perhydrous Indian coals. Int. J. Coal Preparation Util. 30, 62–64.

Kostova, I., Isaeva, E., 2016. Petrography, mineralogy and geochemistry of lignite from stanyantsi basin, Bulgaria. Rev. Bulgarian Geol. Soc. 77 (1), 65–80.

López, I.C., Ward, C.R., 2008. Composition and mode of occurrence of mineral matter in some Colombian coals. Int. J. Coal Geol. 73, 3–18.

Mesroghli, S., Jorjani, E., Chelgani, S.C., 2009. Estimation of gross calorific value based on coal analysis using regression and artificial neural networks. Int. J. Coal Geol. 79, 49–54.

Painter, P.C., Snyder, R.W., Starsinic, M., Coleman, M.M., Kuehn, D.W., Davis, A., 1981. Concerning the application of FT-IR to the study of coal: a critical assessment of band assignments and the application of spectral analysis programs. Appl. Spectrosc. 35, 475–485.

Pickel, W., Kus, J., Flores, D., Kalaitzidis, S., Christanis, K., Cardott, B.J., Misz-Kennan, M., Rodrigues, S., Hentschel, A., Hamor-Vido, M., Crosdale, P., Wagner, N., 2017. Classification of liptinite - ICCP system 1994. Int. J. Coal Geol. 169, 40–61.

Saikia, B.K., Boruah, R.K., Gogoi, P.K., Baruaha, B.P., 2009. A thermal investigation on coals from Assam (India). Fuel Process. Technol. 90, 196–203.

Saikia, B.K., Khound, K., Sahu, O.P., Baruah, B.P., 2015a. Feasibility studies on cleaning of high sulfur coals by using ionic liquids. Int. J. Coal Sci. Techno. 2 (3), 202–210.

Saikia, B.K., Sharma, A., Sahu, O.P., Baruah, B.P., 2015b. Study on physico-chemical properties, mineral matters and leaching characteristics of some Indian coals and fly ash. J. Geol. Soc. India 86, 275–282.

Saikia, B.K., Dutta, A.M., Baruah, B.P., 2014. Feasibility studies of desulphurization and de-ashing of low-grade medium to high sulphur coals by low energy ultrasonication. Fuel 123, 12–18.

Saxby, J.D., Chatfield, P., Taylor, G.H., Fitzgerald, J.D., Kaplan, I.R., Lu, S.T., 1992. Effect of clay minerals on products from coal maturation. Org. Geochem. 18 (Issue 3), 373–383.

Sharma, A., Saikia, B.K., Phukan, S., Baruah, B.P., 2016. Petrographical and thermo-chemical investigation of some North east Indian high sulphur coals. J. Geol. Soc. India 88, 609–619.

Silva, L.F.O., Sampaio, C.H., Guedes, A., de Vallejuelo, S.F.O., Madariaga, J.M., 2012. Multianalytical approaches to the characterisation of minerals associated with coals and the diagnosis of their potential risk by using combined instrumental microspectroscopic techniques and thermodynamic speciation. Fuel 94, 52–63.

Speight, J.G., 1983. The Chemistry and Technology of Coal. Marcel Dekker, New York.

Vassilev, S.V., Vassileva, C.G., 1996. Occurrence, abundance and origin of minerals in coals and coal ashes. Fuel Process. Technol. 48 (Issue 2), 85–106.

Velásquez, B., Mercedes, E., 2016. Coal Production and Economic Growth in the Caribbean Mining Region in Colombia. Revista de Economía del Caribe17, pp. 1–38.

Wilson, M.J., 1994. Clay Mineralogy: Spectroscopic and Chemical Determinative Methods.